Economic Geology
Monograph 10, 1999, pp. 529–540

Finite Element Heat and Fluid-Flow Computer Simulations of a Deep Ultramafic Sill Model for the Giant Kidd Creek Volcanic-Associated Massive Sulfide Deposit, Abitibi Subprovince, Canada

C. Tucker Barrie,†,*

Geological Survey of Canada, 601 Booth Street, Ottawa, Ontario, Canada K1A 0E8

Lawrence M. Cathles, and Alex Erendi

Geology Department, Cornell University, Ithaca, New York 14853

Abstract

The giant Kidd Creek volcanic-associated massive sulfide deposit in the western Abitibi subprovince of Canada is unique in that it is a single deposit rather than one of many in a district, and has a footwall comprising proximal, high-temperature, high silica rhyolites intercalated with komatiite flows. Classic volcanic associated massive sulfide models with a relatively shallow, synvolcanic sill cannot account for its size or singularity. Finite-element heat and fluid-flow computer simulations of a two-dimensional physical model are presented here that can explain how such a deposit could be produced. The physical model has (1) a relatively deep ultramafic sill as the principal heat source, (2) a rhyolite magma conduit that is coincident with a relatively permeable fault, and (3) a less permeable basaltic substrate. All of the computer simulations employ a temperature-dependent, permeability enhancing and reducing thermal cracking front and have a 1.7-km-thick ultramafic sill with its base at 15 km which is set at 1,650°C for 50,000 yr and then allowed to cool.

In the preferred computer simulation, rhyolite magma is injected in the magma conduit episodically during the first 10,000 yr. With these parameters, a single hydrothermal convection cell is established that vents in one location at >200°C for ~650,000 yr, with an average venting temperature of ~300°C and an average venting rate of ~175 cc/cm^2/yr. Venting temperatures and rates drop rapidly thereafter. Approximately 15 million metric tons (Mt) of Cu and Zn in the deposit are provided considering a hydrothermal fluid that precipitates 100 ppm Cu + Zn, a 0.6-km^2 vent area within a catchment graben, and a 22 percent depositional efficiency. The total energy in the hydrothermal fluid expelled is ~1.53×10^{20} cal, or 10.4 MW/km of graben axis. This estimate of hydrothermal energy output per kilometer of rift axis is one-half to two-thirds that of the Taupo volcanic rift zone of New Zealand and about twice that of the average high-temperature hydrothermal flux at the midocean ridge axes.

In the simulations, a thermal cracking front initially forms at the top of the sill at a ~13-km depth, then migrates to a ~8.5-km depth as conductive heat from the sill penetrates into the overlying substrate, and finally collapses down to 13 km as the heat from the sill is mined out. Thus, hydrothermal fluids doubly scour metals from a deep basaltic source region. Thermal cracking also occurs adjacent to and within the rhyolite conduit during and after magma injections, which helps establish hydrothermal venting in one area. Simulations without the rhyolite injections indicate that stable hydrothermal venting at >200°C is delayed by ~100,000 yr and produces ~10 percent less hydrothermal fluid and energy than with the rhyolite injections. Other simulations indicate that higher permeability substrates lead to higher venting rates but with lower venting temperatures and shorter durations. Lower permeability substrates would prevent hydrothermal circulation. This suggests that there is a permeability window for optimal, protracted, high-temperature venting and optimum scavenging of metals from the basaltic substrate.

These computer simulations provide evidence that singular, large volcanic associated massive sulfide deposits of Kidd Creek dimensions can occur where deep ultramafic sills provide heat. The presence of proximal high-temperature, high silica rhyolites which form by partial melting of tholeiitic basalt above the garnet stability field indicates anomalously hot crust possibly related to ultramafic sills and can help delineate vent source areas. Deep, crustal-scale fractures in relatively primitive, ultramafic, or picrite-bearing terrane such as primitive greenstone belts, oceanic plateaus, or thickened oceanic rifts are also favorable locations for voluminous hydrothermal venting and large volcanic associated massive sulfide deposits; such fractures are expected during incipient rifting or mantle plume upwelling in oceanic terrane, away from active midocean rifts.

Introduction

The Kidd Creek volcanic-associated massive sulfide deposit has three geologic features that together make it unique among such deposits worldwide: it is a single orebody rather than one of many in a district, it has komatiite flows intercalated with high silica rhyolites in the footwall stratigraphic succession, and it is very large. Classic models of volcanic associated massive sulfide systems based on high-level subvolcanic intrusions (magma chambers) as

†Corresponding author: email, tubarrie@nrcan.gc.ca
*Alternate address: C.T. Barrie and Associates, Inc., 23 Euclid Ave., Ottawa, Ontario, Canada K1S 2W2.

the principal heat source for ore-precipitating hydrothermal convection are conceptually difficult for Kidd Creek because multiple deposits are expected. For example, the conceptual model of Campbell et al. (1984) envisions the formation of multiple orebodies above large sills (e.g., Noranda "cauldron" setting). Conceptual models of volcanic associated massive sulfide deposits associated with ephemeral, smaller magma chambers at midocean ridge spreading centers produce multiple but much smaller deposits on a scale of tens of kilometers (e.g., Alt, 1995).

The design of this study is to test a physical model that is consistent with the geology of the Kidd Creek volcanic associated massive sulfide deposit using a finite-element heat and fluid flow computer code. The goal is to simulate fluid flow and account for a sufficient mass of metal-precipitating hydrothermal fluids that vent in one location. The physical model is constrained by the mine area geology, by volumetric considerations for a hydrothermal cell large enough to form the deposit, and by the physical parameters of the magmas represented in the footwall. The bulk permeability used for the substrate in the physical model must be assumed and is based on values for similar settings in the literature. In contrast to the classic volcanic associated massive sulfide models, the physical model presented here utilizes a deep heat source in the form of a large ultramafic sill which allows for deeper and more voluminous hydrothermal convection, and a deeply penetrating, relatively permeable fracture-magma conduit that localizes hydrothermal venting in one place.

Geologic Setting

The Kidd Creek mine is located 25 km north of Timmins, Ontario, in the western Abitibi subprovince (Fig. 1). The stratigraphic succession in the immediate Kidd Creek area comprises, from base to top, ultramafic flows and sills (500–1,000 m) in part intercalated with high silica rhyolite flows and tuffs (100–400 m), sulfide-rich ore horizons (0.1–50 m), a locally graphitic, fine-grained siliciclastic unit (2–20 m), gabbro sills (0.3–1 km) and basalt flows, hyaloclastite and breccias (1–2 km). Only ~1.3 km of the footwall stratigraphic succession is preserved in the immediate mine area; however, basalts occur along strike and down section to the east. Regionally, the Kidd-Munro assemblage conformably overlies the 10- to 15-km-thick tholeiitic basalts of the Stoughton-Roquemaure assemblage (T. Barrie and W. Davis, in prep.). Altered ultramafic rock is present ~250 to 350 m down section from ore in the upper levels of the mine and is present within 10 m of the ore at a depth of ~2.5 km. The ore comprises three parallel, elongate lenses that plunge steeply to the north-northwest, at least one of which is known to a depth of >3 km. Ore textures and footwall volcanic textures suggest proximal hydrothermal and felsic magmatic vents (Coad, 1986; Hannington et al., 1999). The ore is within epiclastic, predominantly felsic rocks that reflect deposition in a grabenlike depression, with a graben axis parallel to the ore lenses and extending for at least 3 km. The stratigraphic succession has undergone three principal phases of deformation: D_0, a passive, non-penetrative phase of north-south compression that created east-west fold axes on a regional scale; D_1, an east-northeast-oriented compression, resulting in the west-northwest-trending fold axes and creating a dome and basin-style interference pattern with the D_0 fold axes, and D_2, a northwest-oriented compression, resulting in minor, steep, northeast-plunging fold axes and crenulations. Structural reconstruction of the ore lenses indicates that they were originally stacked, and one intramineralization hiatus is marked by the locally graphitic argillite unit in the hanging wall of the North ore lens and the hanging wall of the South ore lens. Detailed accounts of the stratigraphy, structural geology, footwall komatiite flows, and orebodies are given in Barrie (1999), Bleeker et al. (1999), H.L. Gibson et al. (unpub. data), and Hannington et al. (1999).

A key observation is that high-level sills of any composition are absent in the immediate footwall stratigraphic

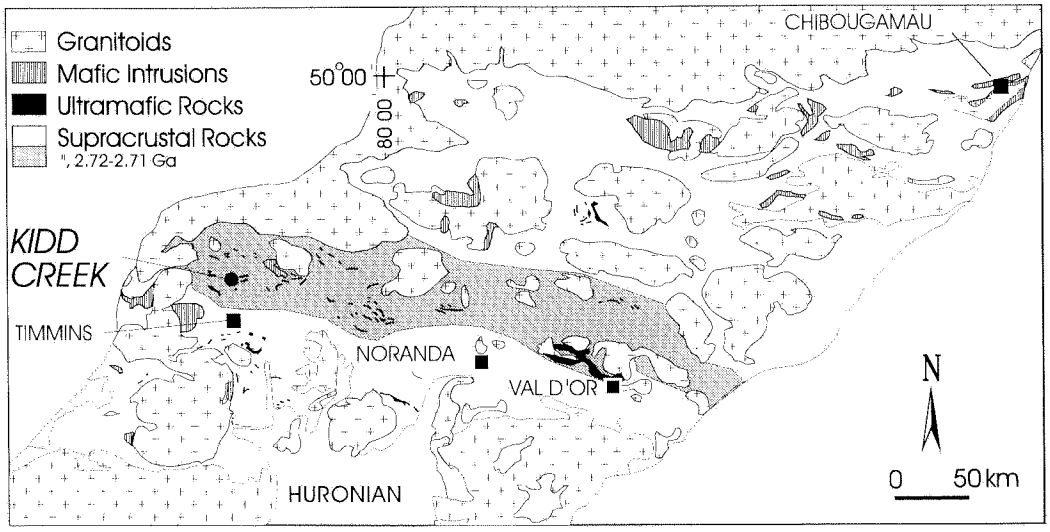

FIG. 1. Location of the Kidd Creek deposit in the Abitibi subprovince, Canada.

succession and along strike for tens of kilometers. The nearest broadly coeval intrusions in the Kidd-Munro assemblage are all ultramafic: a 3- × 4-km intrusive mass 30 km to the west-northwest, several 0.5- to 1-km-thick × 3- to 5-km sills 20 km to the north (north-south compression has contracted the stratigraphic succession by ~50% so this represents a predeformation distance of ~30 km), and the Mann intrusion, a 0.3- to 1.2-km-thick, 40-km mafic-ultramafic sill 55 km to the east-northeast. The absence of a high-level intrusion in the immediate Kidd Creek area is uncommon for the Kidd-Munro assemblage which contains numerous mafic-ultramafic sills (e.g., Dundonald sill, Munro-Warden sill, Ghost Ranges sill, etc.).

Constraints on the Physical Model

The principal geologic features relevant to constructing a physical model for the hydrothermal system that formed the Kidd Creek deposit are (1) the presence of proximal, high silica rhyolites and rhyolitic epiclastic rocks intercalated with komatiite flows in the footwall, (2) volcanic associated massive sulfide ore textures that indicate proximity to a source vent, and (3) a killometer-scale, graben-like depression that contains the orebodies. These features describe an extensional setting that was tectonically and magmatically active immediately prior to mineralization.

Magmatic constraints

A critical constraint comes from the genesis of the high silica rhyolites. The Kidd Creek high silica rhyolites are believed to be the product of partial melting of tholeiitic basalt at relatively shallow levels and at high temperatures (Barrie, 1995). The strong bimodal nature of the volcanic stratigraphic succession precludes their generation by fractional crystallization. The major element composition of the mine rhyolite is similar to ~20 to 25 percent partial melts of an amphibolite of tholeiitic basalt composition, at 900°C and 100 to 300 MPa under dry conditions (Beard and Lofgren, 1991). Melting at higher temperatures or pressures produces melts with too low silica or too high alumina, respectively (Beard and Lofgren, 1991), suggesting that the amphibolite partial melting occurred at ~10 km and possibly under dry conditions. High-temperature, high silica rhyolites like those at Kidd Creek are found in Iceland (Sigurdsson and Sparks, 1981) where there is a very high crustal heat flux (e.g., Ryan, 1990); indeed, their generation requires a high crustal heat flux. At Kidd Creek, the komatiites are intercalated with at least four discrete horizons of high silica rhyolite (Barrie, 1999) indicating that ultramafic magmatism was active at the time of rhyolite generation. Thus a potential heat source for basalt partial melting to form the rhyolites is a relatively deep ultramafic sill. This is consistent with the lack of a high-level ultramafic sill near Kidd Creek, in a volcanic assemblage that contains numerous high-level ultramafic sills, as outlined above.

With these considerations, the physical model presented here has an ultramafic sill with its base at 15-km depth, and a conduit that feeds the proximal footwall rhyolites episodically into a graben-like depression on the paleosea floor (Fig. 2). Ultramafic magmas have perhaps twice as much contained enthalpy as tholeiitic magmas, given the high heat of fusion of forsterite and their high liquidus temperatures (e.g., Sparks, 1987). The ultramafic sill in

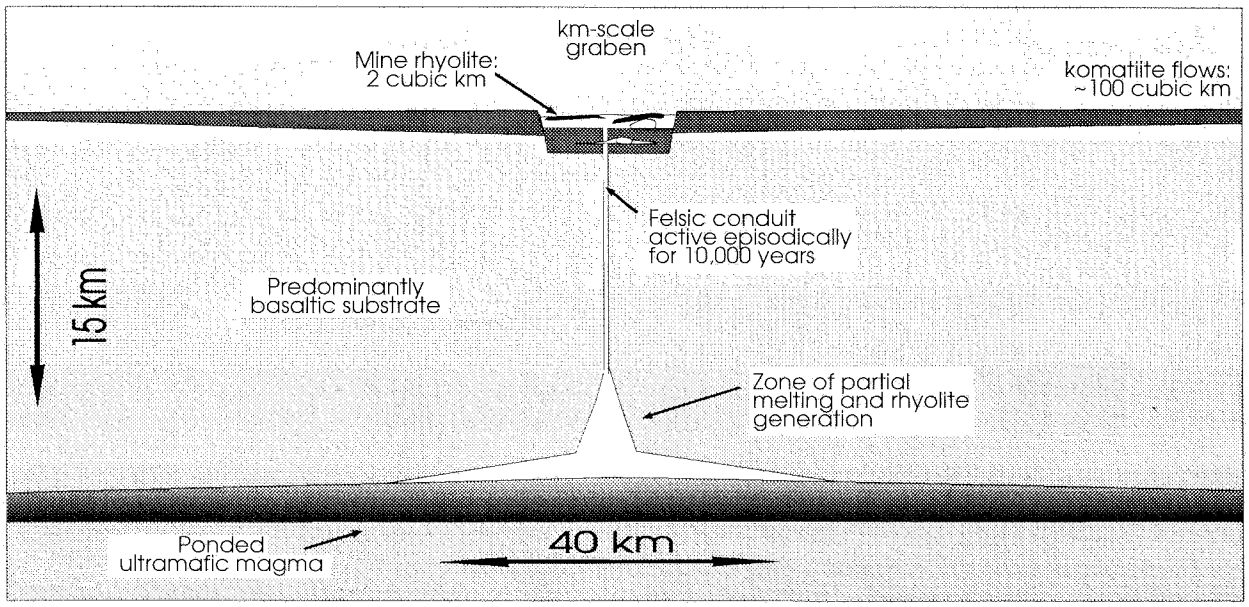

FIG. 2. Schematic two-dimensional diagram for the physical model for the heat and fluid flow simulations. Kidd Creek orebodies in a kilometer-scale graben, with graben axis in and out of plane of diagram. The graben has a 3-km strike length parallel to the orebodies. It contains ~2 km^3 of proximal high silica rhyolite, and ultramafic flows. A predominantly basaltic substrate underlies the graben. An ultramafic sill at 13.3- to 15-km depth extends for 40 km perpendicular to the graben axis. The ponded ultramafic magma partially melts the basaltic substrate to form the high silica rhyolite, which reaches the graben floor through a conduit that is active episodically for 10,000 yr.

the model is 1.7 km thick and 40 km along strike, similar in dimensions to the Mann Township intrusion ~25 km to the east, and only a quarter the size of the Fox River ultramafic sill in northern Manitoba (Scoates and Eckstrand, 1986). It is set at 1,650°C, a reasonable liquidus temperature for a peridotitic ultramafic magma at a 15-km depth (Bickle et al., 1977; Bickle, 1982). The ultramafic sill is maintained at that temperature for 50,000 yr (less than half the time estimated for the crystallization of the Skaergaard intrusion: Norton and Taylor, 1979) and then allowed to cool.

The duration of rhyolite dike injections is estimated considering the volume of footwall mine rhyolite to a depth of 3 km (including stratigraphically equivalent rhyolite adjacent to the north) of ~2 km^3 and the average effusion rate for the Unzen dacite dome, Japan (Nakada et al., 1995) of 3.2×10^5 m^3/d. This yields a period of ~170 yr. There are at least four rhyolite horizons in the footwall, each separated by komatiite flows (Barrie, 1999), with the last the most voluminous. Textures in the intercalated ultramafic flows suggest relatively rapid sequential deposition (Barrie, 1999) consistent with hundreds to thousands of years between komatiite eruptions based on thermal modeling (Gole et al., 1990). Therefore we use four periods of rhyolite dike injection in a feeder conduit for three periods of 25 yr (at 3,000, 5,000, and 7,000 yr) and a final period of 100 yr (at 9,000 yr) during an initial 10,000-yr period. The emplacement temperature for the Kidd Creek rhyolites is based on the zircon geothermometer at 900°C (Barrie, 1995).

Assumptions Regarding Permeability

The substrate and fracture-magma conduit

The substrate beneath the footwall stratigraphic succession preserved at Kidd Creek is predominantly basaltic, because volcanic rocks of the same age and older in the Abitibi subprovince are predominantly mafic. For the physical model, the initial permeability for the substrate is 10^{-16} m^2 (10^{-15} m^2 = 1 mD) horizontally and 5×10^{-17} m^2 vertically. Anisotropy is expected, given the layered nature of a basaltic substrate, and horizontal (flattening) mineral fabric development at a >~10 km depth. The exception is for the area with the 0.5-km-thick, vertical felsic magma conduit, which is given an initial uniform permeability of 10^{-15} m^2. These permeabilities are at the low end of in situ permeabilities measured in basalts of the oceanic crust (drill hole 504 B: 10^{-13}–10^{-17} m^2: Anderson et al., 1985) and at the high end of unfractured igneous rocks (10^{-14}–10^{-21} m^2: Brace, 1980).

Permeability enhancement at a thermal cracking front

For the computer simulations, there is a temperature dependence on permeability that represents a thermal cracking front. Thermal cracking occurs where relatively hot rock is cooled by circulating fluids. Fractures develop during thermal contraction at the interface between conductively heated rocks and rocks cooled by advecting fluid. This phenomenon was first described by Lister (1974) and was later analyzed in detail and modified in the context of the Japanese Kuroko volcanic-associated massive sulfide deposits (Cathles, 1983). In the Kuroko study, it was concluded that permeability must increase with increasing temperature, following Lister's (1974) analysis, and then decrease at higher temperatures due to mineral dissolution along fracture wall irregularities in the presence of a hot hydrothermal fluid. Analysis of venting at midocean ridges indicates that the thermally cracked zone has a significantly higher permeability than estimates of ocean crust from in situ tests (Cathles, 1993, and references therein.). Thermal cracking is supported by field observations in well-preserved mafic intrusions (Manning and Bird, 1986; Schiffries and Skinner, 1987), in ophiolite settings (Nehlig and Juteau, 1988; Everdingen, 1995) and in deep exposures of oceanic crust (Gillis, 1995). In this study, a thermal cracking subroutine increases permeability between 275° and 375°C by two orders of magnitude (from 0.1–10 mD at 375°C for the horizontal permeability in the substrate, or from 1 to 100 mD at 375°C in the relatively permeable fracture) and then decreases it at the same rate with further temperature increases, with the rocks effectively impermeable at >600°C (Fig. 3). This algorithm is similar to one derived for midocean ridge settings that is constrained by measured venting temperatures and rates (Cathles, 1993).

Computer Simulations

The simulations presented here were produced using the program Akcess.basin™, a finite element basin modeling code (Cathles, 1995). They represent the right half of the two-dimensional physical model in Figure 2, with the relatively permeable fracture and felsic magma conduit along the left margin, the ultramafic sill reaching up 1.7 km from the base, and the sea floor at the top (Fig. 4). There are 48 columns and 30 rows of elements, with the majority representing areas 0.5 km wide and 0.33 km

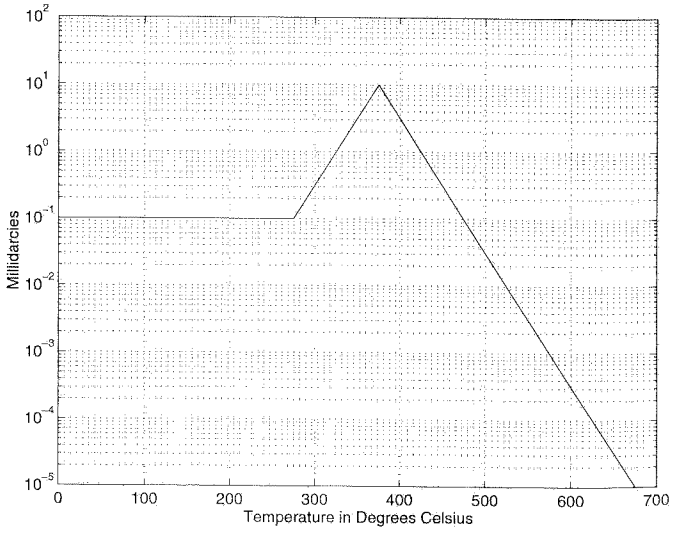

FIG. 3. Permeability vs. temperature for the thermal cracking subroutine.

deep. The widths of the finite elements are refined along the left side that corresponds to the fracture-magma conduit-hydrothermal vent, with four elements at 0.1 km wide along the left side and six elements at 0.25 km wide adjacent and to the left (not resolvable in images in Fig. 4). This refinement makes the simulations more accurate and helps prevent instability. The ultramafic sill has a gradient at the top of ~0.5°, with the shallower end under the relatively permeable fracture. This gradient is geologically reasonable. It assists, but is not required for, the onset of convection and stable convection. The sill remains impermeable after cooling, as expected for hydrated (serpentinized) ultramafic rocks. The sides and bottom of the half cell are insulating and closed to fluid flow, whereas the top is open to fluid flow. This physical model considers a transverse cross section across the graben axial plane. It is recognized that the longitudinal cross section parallel to the graben axial plane would have an important effect on fluid circulation. Such features will be addressed in a subsequent study on the nature of three-dimensional convection in this setting.

The simulations consider one-phase fluid flow. The thermal conductivity used is uniform everywhere at 7×10^{-3} cal/cm-s °C. The basal heat flux is set at 1.05 heat flow units (equal to 10^{-6} calories/cm^2-s) which gives an initial geothermal gradient is 15°C per km depth, a typical value for an oceanic geotherm away from the midocean ridges (Turcotte and Schubert, 1986).

Results

In Figure 4, temperature, permeability, and fluid-flow paths are presented at four times for a simulation that includes rhyolite dike injections at the beginning, at: (1) 10,000 yr, 1,000 yr after the last rhyolite injection in the magma conduit, (2) 50,000 yr, the time when the nodes of the ultramafic sill are unlocked, allowing the sill to cool in the ambient thermal regime, (3) 170,000 yr, when the hydrothermal cell is well established, and (4) 700,000 yr, as the hydrothermal cell begins to wane. At 0 yr, the ultramafic sill is emplaced into the relatively cool basaltic substrate, and thermal cracking is immediately induced in the mafic rocks above the sill at a 13.3-km depth. Convection commences, and erratic venting begins, in the Kidd Creek graben area (upper left in Fig. 4). By 10,000 yr, a hydrothermal convection cell is established. Downwelling occurs for 39.7 of the 40 km of sea floor at the top of the section, with only the three upper left elements (herein termed element 1, at the top of the relatively permeable fracture; and elements 2 and 3, adjacent to the right) venting. The seawater is drawn down to a ~12-km depth within ~1 km of the top of the ultramafic sill through the basaltic substrate which is still relatively cool. This is the interface between substrate heated by conduction from the sill below and the downwelling, modified sea water above, which is the location of the thermal cracking channel. The permeability has increased by ~two orders of magnitude in this area (Fig. 3). In contrast, the permeability has greatly decreased in the fracture due to the episodic injection of rhyolite magma at 900°C, but has increased by one to two orders of magnitude in the adjacent cells to the right due to thermal cracking, thus allowing enhanced venting in element 2, at least temporarily, as governed by the thermal cracking subroutine.

At 50,000 yr (Fig. 4), the base of the hydrothermal cell has risen to a ~11-km depth, and the hydrothermal cell is more established than at 10,000 yr, with steadier venting rates and temperatures. Venting is strongest in element 1 and is an order of magnitude less voluminous in element 2. All of the other top cells represent areas of downwelling on the sea floor. The permeable fracture has cooled sufficiently after the rhyolite injections so that its top 5 km are highly permeable. At 170,000 yr, the base of the hydrothermal cell has risen to 9.5 km, and venting is consistent and strong in element 1 at ~300°C. The hydrothermal cell is now well established. The permeable fracture is heated by advection from a 9.5- to 4-km depth as circulating hydrothermal fluid mines heat from the conductively heated rock below. Fluid within the conduit at this depth interval is at 425° to 350°C but cools to 300°C at the seawater interface due to mixing with cooler fluid drawn into the conduit at shallower levels. Thermal cracking enhances permeability in the cells adjacent to the permeable conduit at a 9.5- to 4-km depth, effectively increasing the width of the conduit at this depth interval.

At 700,000 yr (Fig. 4), the hydrothermal cell is still well established, with venting temperatures and rates comparable to those at 170,000 yr, but the system is about to wane. The base of the hydrothermal cell has dropped to a 11- to 13-km depth, and the temperature of the ultramafic sill has dropped to below 400°C at distance from the magma conduit. Heat from the rocks above the sill is mined out and advected up the fracture. The hydrated (serpentinized) ultramafic sill remains impermeable to the convecting hydrothermal fluids above. By 800,000 yr, a weak secondary cell develops on the right-hand side of the diagram, and venting temperatures and rates drop significantly; the system eventually dies by ~1,000,000 yr.

The history of venting temperatures and rates for element 1 to 1,000,000 yr is recorded in Figure 5. The temperatures in element 1 are erratic during the rhyolite dike intrusions during the first 10,000 yr as they are set at 900°C due to rhyolite dike injection as described above (this time period is not considered in the integrated flux). They drop below 450°C immediately thereafter. The temperatures then plateau at 300° to 305°C at ~115,000 yr and eventually drop below 200°C at 750,000 yr. After 10,000 yr, venting builds from ~25 cc/cm^2/yr to >150 cc/cm^2/yr at ~150,000 yr; then broadly increases to 240 cc/cm^2/yr and drops below 50 cc/cm^2/yr at ~650,000 yr; the average rate for >200°C venting is 175 cc/cm^2/yr. The flux then drops precipitously over the next 100,000 yr, ~50,000 yr before the vent temperature drops. Element 2 follows temperature and flux patterns similar to those of element 1 but with venting rates nearly two orders of magnitude lower than those for element 1.

The total volume of hydrothermal fluid vented for the 0.6-km^2 vent area represented by element 1 (0.1 km wide $\times$ 2 $\times$ 3 km length of graben) is 7.86×10^{17} cc. For

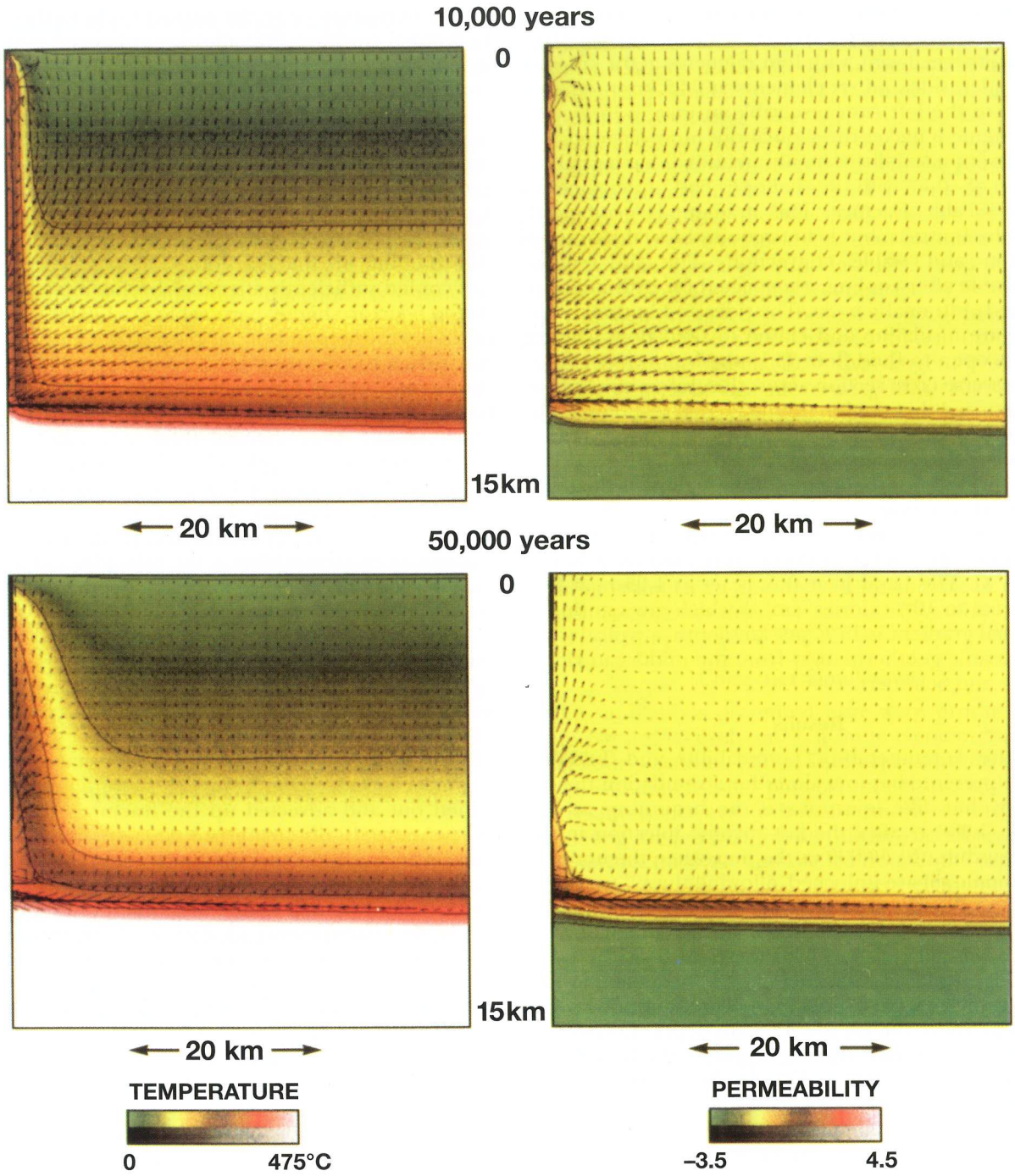

FIG. 4. Temperature and integrated mass flux for 10,000, 50,000, 170,000, and 700,000 yr. These images correspond to the right half of Figure 2. Each image represents half of the total hydrothermal cell 15 km deep and 40 km long. The vectors represent the direction of fluid flow and are proportional to the magnitude of fluid flow, with relative magnification factors of 50, 5, 5, and 2, respectively. The temperature contours are in 100°C intervals, and the permeability contours are in log units.

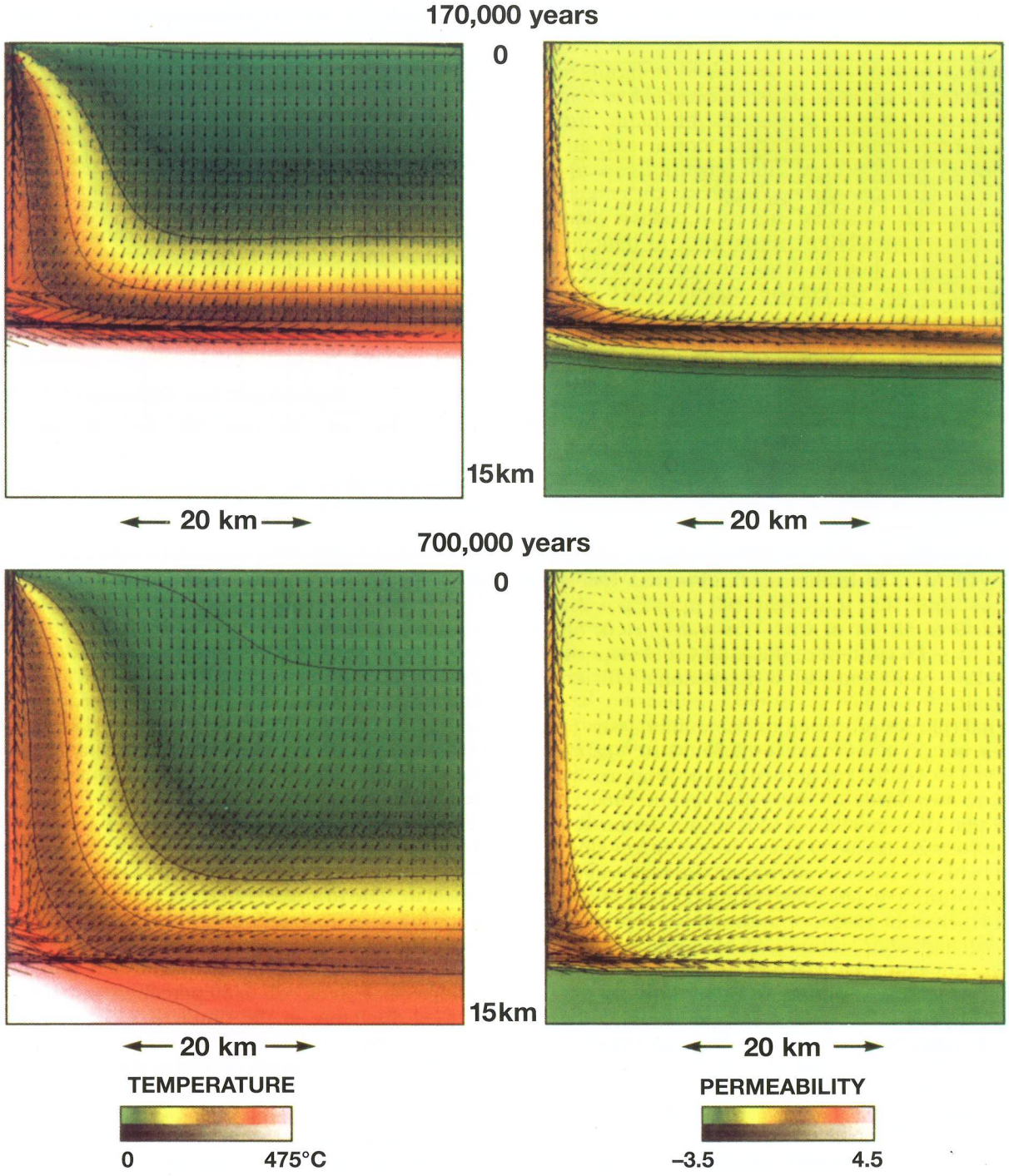
170,000 years
0
15km
20 km
20 km
700,000 years
0
15km
20 km
20 km
TEMPERATURE
0
475°C
PERMEABILITY
–3.5
4.5

FIG. 4. *(Cont.)*

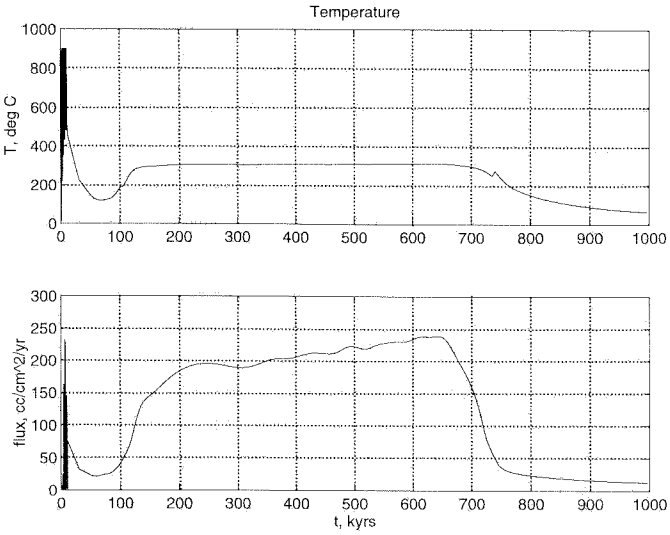

FIG. 5. Temperature for element 1 vs. time (top); venting rate vs. time (bottom). Note that the temperature in element 1 is set at 900°C episodically during the first 10,000 yr, representing rhyolite dike injection.

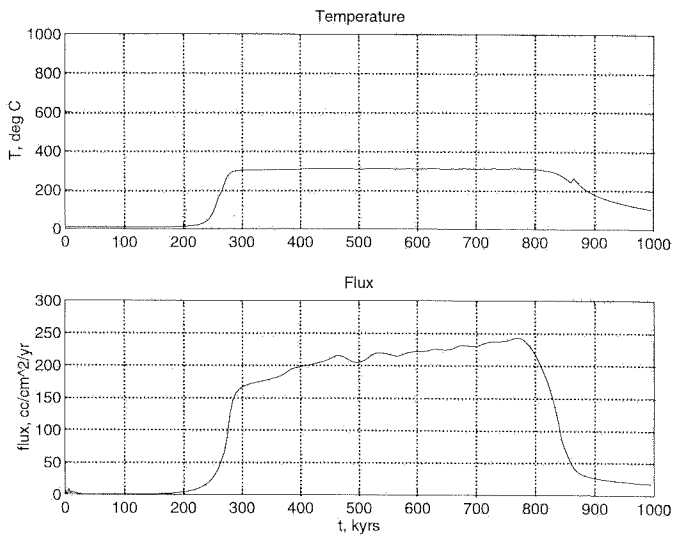

FIG. 6. Venting temperature (top) and venting rate vs. time (bottom) for case study without rhyolite dikes injected along relatively permeable fracture during first 10,000 yr.

>200°C, the volume is 6.84×10^{17} cc, which corresponds to 6.84×10^5 Mt of hydrothermal fluid vented. Using a hydrothermal fluid that transports 100 ppm Cu + Zn, this corresponds to 68 Mt of Cu + Zn transported, or ~4.5 times the Cu + Zn content of the Kidd Creek deposit (~15 Mt Cu + Zn), consistent with a depositional efficiency of ~22 percent.

The total calories produced to one million years for the vent area is 1.53×10^{20} cal, or 7.85×10^{13} cal/km of graben/yr (10.4 MW/km graben). This is approximately one-half to two-thirds of the yearly geothermal energy released per kilometer of rift axis in the Taupo volcanic rift zone, New Zealand (40 km wide × 150 km along the rift axis), which is considered to have the highest geothermal energy output of active arc settings (15–20 MW/km of rift axis: Hochstein, 1995), or approximately twice the average axial, high-temperature hydrothermal output of the midocean ridge systems (per km of rift axis: 40–50 MW total energy per km of midocean ridge, with 65–70% lost by fluid advection [Mottl and Wheat, 1994], of which 10–20% is axial, high-temperature venting [Morton and Sleep, 1985]).

Related computer simulations: The significance of rhyolite dike injections and of permeable fractures

The importance of rhyolite dike injections was investigated by keeping the same parameters as in the simulation above but removing the episodic rhyolite dikes in the first 10,000 yr. The temperature and venting rates versus time are given in Figure 6. Significant venting temperatures and rates in element 1 do not begin until ~250,000 yr, or ~150,000 yr later than the case with rhyolite dikes. The total hydrothermal venting at >200°C and the total energy in the form of hydrothermal venting is ~10 percent less than for the simulation above. The vent temperatures are nearly the same. In a third case, the relatively permeable fracture was removed. In this case, hydrothermal venting was delayed by 100,000 yr, and then eventually occurred in three locations with low temperature and venting rates. The significance of a possible komatiite vent source in the Kidd Creek graben was tested by having five year-long episodes of komatiite magma in the conduit at 1650 to 1500°C, alternating with the rhyolite dikes during the first 10,000 yr. The duration of the komatiite magma injections was estimated assuming that all of the ~100 km^3 contiguous ultramafic rocks erupted from the same conduit as for the rhyolite, using the flow rates for komatiite magma estimated by Huppert and Sparks (1985). The results after ~25,000 yr were nearly identical to the simulation with the rhyolite dikes alone, discussed above. In a fourth case, the width of the rhyolite dike conduit was set at 500 m instead of 100 m. The principal effects were (1) that high-temperature fluids vented earlier, with the system becoming fully established by ~60,000 yr, (2) that there were vent rates of 50 to 60 $cc/cm^2/yr$ for the established part of the hydrothermal system, ~25 to 30 percent lower than the more focused discharge in the simulation above, and (3) that the hydrothermal cell tightened against the dike conduit, with downwelling in all elements but elements 1 and 2, and downwelling fluid migrating toward the conduit more rapidly.

The effect of substrate permeability on the hydrothermal cell was tested in case studies with a less refined finite element grid. It was determined that a tenfold increase in the substrate permeability produced a threefold increase in venting rates but a significant decrease in the average venting temperatures and a much shorter venting duration at >200°C. The effects of substrate permeability for deep ultramafic sill cases has been evaluated in a companion paper (Cathles et al., 1997). Similar effects were noted with a tenfold increase in the relatively permeable fracture. Variations in permeability with depth were considered by assigning a lower permeability to the substrate below 10 km. This had much less of an effect on the system.

The results of these cases indicate that (1) deep, relatively permeable fractures may be required for prolonged high temperature venting using a deep heat source; (2) early, episodic rhyolite dikes are not required to establish hydrothermal venting, but they help establish venting sooner, and they may help produce slightly larger volcanic associated massive sulfide deposits; (3) komatiite feeder dikes have little effect on the hydrothermal system due to their short duration and are no more effective than rhyolite dikes in helping establish the hydrothermal vent area; and (4) there appears to be a permeability window for the substrate that optimizes high venting temperatures and rates, and cracking front scavenging of metals from the basaltic substrate. The optimum permeability window produces a relatively long-lived hydrothermal system.

Discussion and Implications

Constraints on volume and geometry of the source rock

An estimate of the source-rock volume can be made for the Kidd Creek deposit based on contained metal and estimates of leaching and depositional efficiency for comparison with the results of the preferred simulation. The Kidd Creek orebody is known to have contained >149.33 Mt of mined or mineable ore, with an average grade reported for ~130 Mt of 2.89 percent Cu, 6.36 percent Zn, 0.26 percent Pb and 92 g/t Ag, with Sn (0.1% avg), Se, S, and other elements recovered (R. Cook, pers. commun.,1994). This amounts to 4.32 Mt Cu, 9.50 Mt Zn, 0.39 Mt Pb, and 13.7 million kg of Ag; an estimate of the contained sulfur content is 33 Mt (R. Cook, pers. commun., 1994). An estimate of the volume of rock representing the source for the metals can be made using Cu and Zn. Assuming ~15 Mt of ore, Cu and Zn were derived by leaching of rock with ~140 ppm combined Cu and Zn (average composition of 2.70 Ga turbiditic sedimentary rocks 20 km to the south: Feng and Kerrich, 1990), $\sim 5 \times 10^{12}$ t of source rock using 20 percent average leaching efficiency (~12% for Cyprus: 80% leaching over 15% of stratigraphic succession; Richardson et al., 1987) and 10 percent average deposition efficiency (<1–5% for sea-floor systems: Converse et al., 1984; Feely et al., 1994). This corresponds to a source-rock volume of ~1,850 km^3, or a cube ~12 km on a side, using a rock density of 2.7 g/cc. For example, this could be a volume 10 km deep, 3 km parallel to a graben axis (the length of the Kidd Creek orebody), and 61.7 km perpendicular to a graben axis, similar to the dimensions of the physical model considered in this study.

It is difficult to envision a single vent area in a 3-km-long graben above a high-level, synvolcanic intrusion and a source-rock volume of ~1,850 km^3. It can be demonstrated mathematically that for a uniform porous media heated from below, the horizontal distance between two upwelling sites should be twice the thickness of the porous media for hydrothermal convection to commence at the minimum Rayleigh number (Turcotte and Schubert, 1982). Thus a sill at a 3-km depth should have vents at ~6-km spacing and produce at least five volcanic associated massive sulfide deposits. This clearly does not fit the geologic setting at Kidd Creek.

Constraints on the duration of mineralization from U-Pb geochronology

The duration of mineralization at Kidd Creek is constrained by U-Pb zircon ages: 2716.2 ± 1.6 Ma for a concordant, abraded fraction from the East outcrop footwall rhyolite (Barrie and Davis, 1990) and 2711.5 ± 1.2 Ma for the quartz porphyry unit in the mine hanging wall (Bleeker et al., 1999). The three main ore lenses were originally stacked, with one hiatus of unknown duration documented by a turbiditic, sulfidic argillite that is continuous from above the North orebody to below the South orebody. The U-Pb ages bracket the mineralization event to ~5 m.y., or a minimum of 1.9 m.y. considering the 2σ errors. The preferred simulation presented here is within an order of magnitude of these constraints, with venting at >200°C for ~650,000 yr.

Deep hydrothermal convection and volcanic associated massive sulfide deposits

The preferred computer simulation of the physical model presented here is consistent with the contention that volcanic associated massive sulfide-forming hydrothermal systems can penetrate 10 to 15 km into the crust, in contrast to the established paradigm that volcanic associated massive sulfide systems require a high-level, subvolcanic intrusion (magma chamber) as a heat source (e.g., Campbell et al., 1984) with much shallower hydrothermal convection. Elsewhere, evidence for deeper convection comes from seismic and resistivity surveys, isotopic studies, and direct observations, in addition to numerical modeling. Seismic and resistivity surveys in continental settings indicate that hydrostatic conditions (e.g., water hydraulically connected to the surface: "free water") are common in the crust to 10 to 12 km (Nur and Walder, 1990). In oceanic settings near the midocean ridges, microseismic activity has been detected to 8- to 10-km depths and is considered to reflect cracking of the oceanic crust by hydrothermal fluid migration (McClain et al., 1993). Away from the ridges, seismic profiles indicate major fault systems that ruptured the crust to depths of 8 to 10 km (Morris et al., 1993). Oxygen isotope studies of mafic and felsic intrusions indicate massive hydrothermal fluid fluxes to depths of 10 to 15 km, particularly in rifted tectonic settings (Taylor and Forester, 1979; Taylor, 1990). Lead isotope signatures of massive sulfide at the Navan Pb-Zn deposit, Ireland, indicate that hydrothermal fluids transported metals from a basement 10 to 12 km below the upper lenses (Mills et al., 1987). Field observations document high (600°–>700°C) and moderate temperature (250°–400°C) vein and fracture systems within and near the margins of the Bushveld Complex, South Africa, across a stratigraphic thickness of 9 km and a strike length of >100 km, and to paleodepths of ~15 km (Shiffries and Rye, 1990).

The ultimate lower limit of volcanic associated massive sulfide-related hydrothermal convection is probably the brittle-ductile transition, which is dependent on the geothermal gradient and the composition of the rock types.

The presence or absence of quartz plays a major role, as quartz is more plastic than most other rock-forming minerals and deforms by dislocation creep at temperatures as low as ~300°C (Tullis and Yund, 1977). Given the proper circumstances—a rift-related setting with abundant crustal-scale faulting and fracturing, a relatively low initial geothermal gradient, a quartz-poor crustal substrate, and a large heat source at depth in the form of a mafic or ultramafic intrusion—volcanic associated massive sulfide-related hydrothermal convection can penetrate to depths of 10 to 15 km.

The permeability window for long-lived, high-temperature venting

There appears to be an optimal crustal permeability, or permeability window, for long-lived, voluminous high-temperature venting required to form the Kidd Creek volcanic associated massive sulfide deposit. In simulations of similar physical models run early in the course of this study, it would appear that the bulk crustal permeability required for scavenging and related high-temperature venting is within half an order of magnitude of ~10^{-16} m^2; higher permeabilities lead to lower venting temperatures due to more mixing between deep, hot fluid with cooler fluid closer to the sea floor, higher venting rates, and shorter durations. Low permeabilities cut off convection. The constraints of bulk crustal permeability on other volcanic associated massive sulfide systems with different metal budgets and geologic constraints remains to be fully explored.

Importance of felsic conduits

Magma conduits tend to seek more permeable fractures or faults through the crust and thus mark the location of potential hydrothermal conduits, and they also can enhance the permeability within and adjacent to fractures due to thermal cracking, as demonstrated here. Felsic and mafic magma conduits have the potential to help establish hydrothermal convection and pin the vent area in one location. Ultramafic magmas, although much hotter than other magma types, have short eruption periods on the order of weeks or months, and they may thermally erode the wall rocks at a rate comparable to thermal conduction (Huppert and Sparks, 1985); thus, ultramafic magmas may be inefficient at establishing hydrothermal vent areas. Voluminous eruptions that produce flood basalt or oceanic plateau provinces have the duration necessary to establish strong hydrothermal convection in one location. However, flood basalts may pond thickly above vent sources and extinguish hydrothermal cells. Rhyolite eruptions that feed flow domes are on the order of tens of yr and thus have the duration to help establish hydrothermal vent areas, as demonstrated in this study. This may explain the close association of volcanic associated massive sulfide deposits with rhyolite domes in the kuroko district (e.g., Sato, 1974) and in many other areas: the felsic conduit helps lock hydrothermal venting in one place, and the location for the venting is marked by the proximal rhyolite dome at the top of the conduit.

Significance for volcanic associated massive sulfide exploration

The giant Kidd Creek deposit presents an attractive exploration target, and this deep ultramafic sill physical model provides an alternative to conventional volcanic associated massive sulfide models for base exploration in ultramafic-rich terrane. Kidd Creek is within the Kidd-Munro assemblage, which is correlatable with the ultramafic-rich Stoughton-Roquemaure and Lower Malartic Groups in the southeastern Abitibi subprovince. The presence of proximal, high-temperature high silica rhyolites in these areas would indicate regions where sufficient heat has penetrated the crust to cause partial melting of tholeiitic basalts above the garnet stability field; if the heat sources were ultramafic, then the conditions would be similar to those at Kidd Creek. The relatively large hydrothermal cell in this physical model suggests that coeval stratigraphic successions near the Kidd Creek deposit are likely to be areas of downwelling, rather than vent sites, although subsidiary hydrothermal systems are possible.

Other volcanic terranes with a significant ultramafic component: the Circum-Superior belt, Canada, the Zimbabwe craton, the Barberton and Murchison greenstone belts of the Kaapvaal craton, South Africa, the Kambalda area of the Norseman-Wiluna belt, and Western Australia, should be considered for volcanic associated massive sulfide deposit potential, in light of this study. On a crustal scale, the Kidd-Munro and correlatable assemblages in the southern Abitibi subprovince show no evidence of the presence of an older crustal substrate at the time of their formation, based on Nd, Pb, and Hf isotope signatures (Corfu and Noble, 1992; Barrie et al., 1999, and references therein) and a lack of zircon inheritance (Corfu, 1993), consistent with the highly primitive nature. In this respect the primitive Circum-Superior belt is similar to the Kidd-Munro assemblage, and it contains volcanic associated massive sulfide deposits; however, many of the other ultramafic areas have older cratonic roots and are volcanic associated massive sulfide poor. Older cratonic roots may be too impermeable and thus inhibit deep volcanic associated massive sulfide-forming hydrothermal systems associated with deep ultramafic sills.

Conclusions

The preferred simulation for the physical model presented here accounts for the metal budget of the largest and arguably the most valuable volcanic associated massive sulfide deposit known in the world. The physical model is consistent with the broad geologic features of the Kidd Creek volcanic associated massive sulfide deposit. This study considers modified sea water (modified connate water initially) as the metal-transporting agent and a basaltic substrate as the metal source region. This study presents a conceptual model significantly different from the current paradigm for the formation of volcanic associated massive sulfide deposits related to shallow subvolcanic intrusions. A deep, ultramafic intrusion is used as the principal heat source. It suggests that volcanic associated massive sulfide-forming hydrothermal convection

can penetrate deeply into the crust, leach metals from a large source region, and bring them to a single vent site on the sea floor. The concept of thermal cracking (and resealing at high temperatures) is validated through this and previous studies on volcanic associated massive sulfide systems (e.g., Cathles, 1983), since the venting and energy budget necessary to reproduce the deposits requires temperature-dependent permeability enhancement and reduction. The significance of rhyolite magmatism spatially associated with volcanic associated massive sulfide deposits in bimodal volcanic terrane is highlighted here: rhyolite conduits along relatively permeable fractures help establish hydrothermal venting early in the evolution of a hydrothermal cell, and proximal rhyolite flow domes may coincide with the location of the hydrothermal vent. Further analysis of magmatic heat-driven volcanic associated massive sulfide systems using this approach will provide further constraints on kilometer-scale substrate and fracture permeability, which will be used in turn for more detailed analysis of Kidd Creek and other volcanic associated massive sulfide systems.

Acknowledgments

This study has been partially supported by Kidd Creek Mines Ltd., Falconbridge Exploration Ltd., the Global Basin Research Network, and the Northern Ontario Development Agreement between Ontario and the Federal government of Canada. We thank M. Hannington and I. Jonasson for discussions on this topic, *Economic Geology* referees for their comments, and J. Shosa for assistance with computer graphics.

REFERENCES

Anderson, R.N., Zoback, M.D., Hickman, S.H., and Newmark, R L., 1985, Permeability versus depth in the upper oceanic crust: In situ measurements in DSDP hole 504B, eastern equatorial Pacific: Journal of Geophysical Research, v. 90, p. 3659–3669.

Barrie, C.T., 1995, Zircon thermometry of high-temperature rhyolites near volcanic-associated sulfide deposits, Abitibi subprovince, Canada: Geology, v. 23, p. 169–172.

——1999, Komatiite flows of the Kidd Creek footwall, Abitibi subprovince, Canada: Economic Geology Monograph 10, p. 143–162.

Barrie, C.T., and Davis, D.W., 1990, Timing of magmatism and deformation in the Kamiskotia-Kidd Creek area, western Abitibi subprovince, Canada: Precambrian Research, v. 46, p. 217–240.

Barrie, C.T., Cousens, B.L., Hannington, M D., Bleeker, W., and Gibson, H.L., 1999, Lead and neodymium isotope systematics of the Kidd Creek mine stratigraphic sequence and ore, Abitibi subprovince, Canada: Economic Geology Monograph 10, p. 497–510.

Beard, J.S., and Lofgren, G E., 1991, Dehydration melting and water-saturated melting of basaltic and andesitic greenstones and amphibolites at 1, 3, and 6.9 kb: Journal of Petrology, v. 32, p. 365–401.

Bleeker, W., 1999, Structure, stratigraphy, and primary setting of the Kidd Creek volcanogenic massive sulfide deposit: A semiquantitative reconstruction: Structure, stratigraphy and geochronology of the Kidd Creek volcanic complex: Economic Geology Monograph 10, p. 71–122.

Brace, W.F., 1980, Permeability of crystalline and argillaceous rocks: Status and problems: International Journal of Rock Mechanics in Mineral Science and Geomechanical Abstracts v. 17, p. 876–893.

Campbell, I.H., Franklin, J.M., Gorton, M.P., and Hart, T.R., 1981, The role of subvolcanic sills in the generation of massive sulfide deposits: Economic Geology, v. 76, p. 2248–2253.

Cathles, L.M., 1983, An analysis of the hydrothermal system responsible for massive sulfide deposition in the Hokurolu basin of Japan: Economic Geology Monograph 5, p. 439-487.

——1995, The Akcess.basin finite element simulation code: U.S. Department of Energy Report, 614 p.

Cathles, L.M., Erendi, A.H.J., and Barrie, C.T., 1997, How long can a hydrothermal system be sustained by a single intrusive event?: Economic Geology, v. 92, p. 766–771.

Coad, P.R., 1985, Rhyolite geology at Kidd Creek: A progress report: Canadian Institute of Mining and Metallurgy Bulletin, v. 78, p. 70–83.

Converse, D.R., Holland, H D., and Edmond, J M., 1984, Flow rates in the axial hot springs of the East Pacific Rise (21° N): Implications for the heat budget and the formation of massive sulfide deposits: Earth and Planetary Science Letters, v. 69, p. 159–175.

Corfu, F., 1993, The evolution of the southern Abitibi greenstone belt in light of precise U-Pb geochronology: Economic Geology, v. 88, p. 1323–1340.

Corfu, F., and Noble, S.R., 1992, Genesis of the southern Abitibi greenstone belt, Superior province, Canada: Evidence from zircon Hf-isotope analyses using a single filiment technique: Geochimica et Cosmochimica Acta, v. 56, p. 2081–2097.

Feely, R.A., Massoth, G.J., Trefry, J.H., Baker, E.T., Paulson, A.J., and Lebon, G.T., 1994, Composition and sedimetation of hydrothermal plume particles from North Cleft segment, Juan de Fuca Ridge: Journal of Geophysical Research, v. 99, p. 4985–5006.

Feng, R., and Kerrich, R., 1990, Geochemistry of fine-grained clastic sediments in the Archean Abitibi greenstone belt, Canada: Implications for provenance and tectonic setting: Geochimica et Cosmochimica Acta, v. 54, p. 1061–1081.

Gillis, K.M., 1995, Controls on hydrothermal alteration in a section of fast-spreading oceanic crust: Earth and Planetary Science Letters, v. 134, p. 473–489.

Gole, M.J., Barnes, S J., and Hill, R.E.T., 1990, Partial melting and recrystallization of Archean komatiites by residual heat from rapidly accumulated flows: Contributions to Mineralogy and Petrology, v. 105, p. 704–714.

Hannington, M.D., Jonasson, I.R., Herzig, P.M., and Peterson, S., 1995, Physical and chemical processes at midocean ridges: American Geophysical Union Geophysical Monograph 91, p. 115–157.

Hannington, M.D., Bleeker, W., Kjarsgaard, I., 1999, Sulfide mineralogy, geochemistry and ore genesis of the Kidd Creek deposit, Part I: North, central, and South orebodies: Economic Geology Monograph 10, p. 163–224.

Hendley, R.W., and Roberts, P., 1983, Epithermal environments in New Zealand: New Zealand Mineral Exploration Association Field Conference Guidebook, 80 p.

Hill, R.E T., Gole, M.J., and Barnes, S.J., 1987, Physical vocanology of komatiites: A field guide to the komatiites between Kalgoorlie and Wiluna, Eastern Goldfields province, Yilgarn block, Western Australia: Geological Society of Australia, Western Australia Division, Excursion Guide Book, 74 p.

Huppert, H E., and Sparks, R S.J., 1985, Komatiites I: Eruption and flow: Journal of Petrology, v. 26, p. 694–725.

Huston, D., and Taylor, B E., 1999, Genetic significance of oxygen and hydrogen isotope variations at the Kidd Creek volcanic-hosted massive sulfide deposit, Ontario, Canada: Economic Geology Monograph 10, p. 335–350.

Lister, C.R B., 1974, On the penetration of water into hot rock: Royal Astronomical Society Geophysical Journal, v. 39, p. 465–509.

Manning, C.E., and Bird, D.K., 1987, Hydrothermal clinopyroxenes of the Skaergaard intrusion: Contributions to Mineralogy and Petrology, v. 92, p. 437–447.

McClain, J.S., Begnaud, M.L., Wright, M.A., Fondrk, J., and von Damm, G.K., 1993, Seismicity and tremor in a submarine hydrothermal field: The northern Juan de Fuca ridge: Geophysical Research Letters, v. 20, p. 1883–1886.

Mills, H., Halliday, A.N., Ashton, J.H., Anderson, I K., and Russell, M.J., 1987, Origin of a giant orebody at Navan, Ireland: Nature, v. 327, p. 223–226.

Morris, E., Detrick, R.S., Minshull, T.A., Mutter, J C., White, R.S., Su, W., and Buhl, P., 1993, Seismic structure of oceanic crust in the western North Atlantic: Journal of Geophysical Research, v. 98, p. 13879–13903.

Nakada, S., Miyake, Y., Sato, H., and Fujinawa, A., 1995, Endogenous growth of dacite dome at Unzen volcano (Japan), 1993–1994: Geology, v. 23, p. 157–160.

Nehlig, P., and Juteau, T., 1988, Flow porosities, permeabilities and preliminary data on fluid inclusions and fossil thermal gradients in the crustal sequence of the Sumail ophiolite (Oman): Tectonophysics, v. 151, p. 199–221.

Nur, A.M., and Wader, J., 1990, Time-dependent hydraulics of the earth's crust, *in* The Role of Fluids in Crustal Processes, Studies in Geophysics, National Research Council: Washington, D.C., National Academy Press, p. 113–127.

Richardson, C.J., Cann, J.R., Richards, H.G., and Cowan, J.G., 1987, Metal-depleted root zones of the Troodos ore-forming hydrothermal systems, Cyprus: Earth and Planetary Science Letters, v. 84, p. 243–253.

Ryan, M.P., 1990, The physical nature of the Icelandic magma transport system, *in* Ryan, M.P., ed., Magma Transport and Storage: New York, John Wiley and Sons, p. 176–224.

Sato, T., 1974, Distribution and geologic setting of the kuroko deposits: Society of Mining Geologists of Japan Special Issue 6, p. 1–9.

Schiffries, C.M., and Rye, D M., 1990, Stable isotopic systematics of the Bushveld Complex: II. Constraints on hydrothermal processes in layered intrusions: American Journal of Science, v. 290, p. 209–245.

Schiffries, C.M., and Skinner, B.J., 1987, The Bushveld hydrothermal system: Field and petrologic evidence: American Journal of Science, v. 287, p. 566–595.

Scoates, R.F.J., and Eckstrand, O.R., 1986, Platinum-group elements in the upper central layered zone of the Fox River Sill, Northeastern Manitoba: Economic Geology, v. 86, p. 1137–1146.

Sigurdsson, H., and Sparks, R S.J., 1981, Petrology of rhyolitic and mixed magma ejecta from the 1875 eruption of Askja, Iceland: Journal of Petrology, v. 22, p. 41–84.

Sparks, R.S.J., 1986, The role of crustal contamination in magma evolution through geologic time: Earth and Planetary Science Letters, v. 78, p. 211–223.

Taylor, H.P., Jr., 1990, Oxygen and hydrogen isotope constraints on the deep circulation of surface waters into zones of hydrothermal metmorphism and melting, *in* The Role of Fluids in Crustal Processes, Studies in Geophysics, National Research Council: Washington, D.C., National Academy Press, p. 72–95.

Taylor, H.P., Jr., and Forester, R.W., 1979, An oxygen and hydrogen isotope study of the Skaergaard intrusion and its country rocks: A description of a 55-m.y.-old fossil hydrothermal system: Journal of Petrology, v. 20, p. 355–419.

Turcotte, D.L., and Schubert, G., 1982, Geodynamics: Application of continuum physics to geological problems: New York, John Wiley and Sons, 450 p.

Tullis, J., and Yund, R.A., 1977, Experimental deformation of dry Westerly Granite: Journal of Geophysical Research, v. 82, p. 5705–5718.

van Everdingen, D.A. 1995, Fracture characteristics of the sheeted dike complex, Troodos ophiolite, Cyprus: Implications for permeability of oceanic crust: Journal of Geophysical Research, v. 100, p. 19957–19972.